CHAPTER 1

Introduction

Raising interest in research and industrial use of quantum technologies trigger the need of compact, efficient, robust and narrow spectral linewidth laser sources. Distributed feedback (DFB) and distributed Bragg (DBR) lasers are suitable laser types to match these requirements due to their monolithically integrated frequency selective grating as well as the ability to process them on wafer level scale. GaAs-based lasers are able to access transitions in alkali vapors, e.g. transitions in Rb and Cs at 778 nm, 780 nm, 795 nm 852 nm and 894 nm [ISS95] directly enabling e.g. compact frequency references based on macroscopic optics [New+19; Str+21] or even based on integrated photonic circuits [Gal+23]. At the same time these devices are suitable to be used as sources for classical metrology applications needing highly coherent light. Although DFB diode lasers were described [KS72] and demonstrated [SBS74] more than 50 years ago, newly developed DFB lasers, especially at wavelengths near to transitions in alkali metals, are continued to be published [Vir+18; Zha+19; Di +20; Ulk+23; Di +24]. Also the Ferdinand-Braun-Institut (FBH) developed GaAs-based high-power DFB diode lasers suitable to reach these wavelengths [Wen+02; Wen+04a; Wen+04b; Spi+10; Ngu+12; Bro+14].

Besides accessing selected wavelengths, often also a stable single mode emission is necessary. This includes avoiding mode hops during operation, i.e. the switching of longitudinal modes which lead to noncontinuous wavelength changes under continuously altered operation conditions. Most obviously, measurement signals deduced from the absorption at the spectral transitions may become discontinuous or even disappear, i.e. circumventing measurements and disturbing control loops of the systems in which the laser are integrated strongly. In addition, mode hops are known to be accompanied by increased intensity noise [HC93] deteriorating the noise budget in any system the lasers are used in.

In principle, DFB lasers can provide mode-hop-free tuning over a broad range of operating conditions, i.e. the injection current and the operating temperature, since the feedback for the resonator is provided by the grating along the complete laser cavity in contrast to DBR lasers which show longitudinal mode hops when operating conditions are changed due to a varying rise in temperature in the different sections of the devices [Rad+11]. Additionally, DBR lasers tend to distinct multi mode emission around mode hops [Tro+18]. However, DFB lasers with ideally uniform gratings support two degenerate longitudinal modes [KS72]. Stable single mode emission can be established in DFB lasers by integrating a phase shift to the otherwise uniform grating [Uta+84]. Another ansatz to provide single mode emission is to use DFB lasers with highly reflective (HR) coated rear facets [SBS75; Hen85] which corresponds to integrating a phase shift at the rear facet as well. The exact rear facet phase (RFP) is defined by the position of the facet with respect to the Bragg grating and cannot be controlled effectively during processing with a precision clearly below the grating period of a few 100 nm. Thus, the actual RFP condition is randomly distributed which influences the emission properties of the DFB lasers and includes the occurrence of mode hops above threshold. Beside the benefits of a high optical output power at a short resonator length this design requires the characterization and selection of suitable devices if e.g. mode-hop-free tuning is necessary. Although there exist investigations on HR-AR coated DFB lasers to estimate the amount of devices that provide stable single mode emission for varying phase conditions [Buu86; GM87; Ish+87; KM89] partly based on phenomenological assumptions no comprehensive analysis for the occurrence of mode hops in such high-power DFB lasers far above threshold is published. This is in contrast to well established investigations for DBR lasers [Rad+11] and DFB lasers with integrated phase shift and anti-reflective (AR) coated facets [Whi+89] or in DFB lasers with multiple integrated phase shifts [Hil+94b; Hil+94c] which include thorough analysis of the wavelength tuning behavior and explanations for the occurrence of mode hops above threshold, respectively. In reference [Fan+97] the longitudinally varying optical intensity profile along the resonator and its influence on the longitudinally varying carrier density is investigated above threshold for HR-AR coated DFB lasers. Self-consistent numerical simulations as well as experimental data are presented for selected RFP conditions with good agreement. Based on these results theoretical predictions are made which RFP conditions lead to mode hops above threshold. Unfortunately, the longitudinal optical intensity profile and the longitudinal carrier density profile is not given for all RFP conditions, especially not at RFP conditions where mode hops occur nor any explicit spectral data is presented around mode hops. Thus, the spectral behavior above threshold is described self-consistently, neglecting a longitudinally varying temperature profile along the short resonator length. However, concrete mechanisms which lead to mode hopping above threshold remain not well-understood. Beside a more thorough knowledge of the lasers this would be worthwhile since understanding the spectral behavior of the lasers potentially opens up the opportunity to identify and distinguish other factors that limit the single mode emission of the lasers more easily and possibly identify devices showing mode hops more efficiently.

Objective of this work

This thesis focuses on the investigation of the spectral behavior of GaAs-based high-power DFB lasers developed at FBH [Bro+14], especially a better understanding of the spectral tuning behavior and the occurrence of mode hops in devices with HR coated rear facets for specific RFP conditions. This includes numerical simulations as well as experimental tests of the theoretical findings. The work of [Fan+97] points out a possible way to gain more insight into the spectral behavior of HR-AR coated DFB lasers if all RFP conditions are considered. Thus, a suitable numerical software suite, BALaser [Rad24], is used to describe the behavior of HR-AR coated DFB lasers above threshold which includes a corresponding model for the optical intensity and the carrier density profile along the DFB laser resonator. In addition, it allows for considering self-heating of the devices self-consistently. Preferentially, devices emitting at a wavelength around 780 nm are analyzed. Moreover, DFB laser designs are tested that are intended to provide mode-hop-free tuning for a wide range of operation conditions. This includes tests of high-power DFB lasers with integrated phase shift and AR coated facets.

Structure of this work

The work is structured as follows: After a short presentation of basic concepts for laser diodes providing longitudinal single mode emission in Ch. 2 methods for modeling laser diodes are reviewed in Ch. 3. In the following these methods are used to describe the behavior of DFB lasers. The experimental setup used to characterize the laser diodes is presented in Ch. 4. DFB laser with HR coated rear facet are investigated in Ch. 5. First, numerical simulations on the tuning behavior as well as experimental data to test the simulation results are given. Based on these results the mounting technology and its influence on the spectral behavior of the DFB lasers is investigated. The chapter is closed with an analysis of a DFB laser with a HR coated rear facet and an adaptable RFP section. On the one hand it is demonstrated that the device is able to control the occurrence of mode hops or rather make those devices mode-hop-free tunable within a reasonable operating range. On the other hand the device is used to additionally test the simulation results from the beginning of the chapter. DFB lasers with AR coated facets and a QWPS are investigated in Ch. 6. These devices are based on the lasers presented in Ch. 5. After a first demonstration of the successful integration of QWPS's in the middle of otherwise uniform DFB gratings the emission characteristics, including mode-hop-free tuning of the devices, is analyzed. Based on first results, an optimized DFB laser design with tilted ridge is presented and characterized as well as further optimizations for the specific laser design are discussed. Results of the work are already partly publicated. This includes the numerical simulations of the spectral behavior of HR-AR coated DFB lasers [Reg+23] as well as the analysis of HR-AR coated DFB lasers with an adaptable RFP section [Reg+24b] in Ch. 5. Furthermore, results of the AR-AR coated DFB lasers with QWPS and tilted ridge from Ch. 6 are presented in [Reg+24a].

CHAPTER 2

Longitudinal single mode operation of laser diodes

This chapter reviews concisely a selection of well established edge emitting diode laser types and systems which allow for longitudinal single mode operation at a single wavelength or frequency starting with Fabry-Perot (FP) type laser diodes which do not necessarily support only one longitudinal mode. Special focus is laid on the tuning behavior when operation conditions like the temperature or the injection current are altered. DFB lasers are introduced more thoroughly to lay down the fundamentals for the following chapters. All laser types discussed are expected to operate on a single lateral mode, i.e. it exists a sufficient confinement that supports only the fundamental mode. This can be achieved e.g. by introducing an appropriate RW [Lee+75] to the devices.

2.1 Fabry-Perot type lasers

The resonator of FP type lasers consists of semiconductor material which provides optical gain when an electrical current is injected and the cleaved facets forming the mirrors of the resonator. HR and AR dielectric coatings may be applied to the facets to provide higher optical output from only one of the facets. Assuming that a plane wave travels longitudinally in z direction within the resonator the wave can be described by

$$E(z) = E_0 \mathrm{e}^{\mathrm{i}(\omega_0 t - \beta z)} \tag{2.1}$$

where E_0 is the amplitude of the wave, $\omega_0 = 2\pi\nu_0$ the angular frequency with the frequency ν_0, at the point in time t and

$$\beta = \frac{2\pi n_{\mathrm{eff}}}{\lambda_0} + \mathrm{i}\frac{g - \alpha_0}{2} \tag{2.2}$$

the propagation constant of the mode at the wavelength λ_0 which sees the effective index n_{eff}. The mode may experience modal gain g or losses α_0 during propagation. From basic laser physics follows that claiming the amplitude and phase to match after one round trip in the resonator of length L and facet mirrors with reflectivity r_{front} and r_{rear} results in [CCM12]

$$r_{\mathrm{front}} r_{\mathrm{rear}} \mathrm{e}^{-\mathrm{i}2\beta L} = 1\,. \tag{2.3}$$

Thus, two lasing conditions follow. On the one hand the modal gain must reach the level of losses at threshold $g \equiv g_{\mathrm{th}}$ to satisfy the real part of Eq. (2.3)

$$g_{\mathrm{th}} = \alpha_0 + \frac{1}{L} \ln \left(\frac{1}{r_{\mathrm{front}} r_{\mathrm{rear}}} \right) \equiv \alpha_0 + \alpha_m \tag{2.4}$$

where α_m can be identified as mirror losses. Here, the reflectivity of the facets is assumed to be real valued. On the other hand from the phase condition follows at threshold by satisfying the imaginary part of Eq. (2.3)

$$\Re\{\beta\} L = m\pi \tag{2.5}$$

with m being an integer. I.e. the lasing condition is fulfilled at several wavelengths $\lambda_0 = 2 n_{\mathrm{eff}} L/m$. Accordingly, the distance in wavelength $\Delta\lambda$ between adjacent modes is [CCM12]

$$\Delta\lambda = \frac{\lambda_0^2}{2 n_{\mathrm{g}} L} \tag{2.6}$$

with n_{g} being the group index by allowing for dispersion

$$n_{\mathrm{g}} = n_{\mathrm{eff}} - \lambda \frac{\partial n_{\mathrm{eff}}}{\partial \lambda} \,. \tag{2.7}$$

Using $\lambda_0 = c_0/\nu_0$ where c_0 is the speed of light it follows from Eq. (2.6) that the distance in frequency $\Delta\nu$ between adjacent modes is

$$\Delta\nu = \frac{c_0}{2 n_{\mathrm{g}} L} \,. \tag{2.8}$$

Assuming a resonator length of $L = 1500\,\mu\mathrm{m}$ and a group index of approximately $n_{\mathrm{g}} = 4$[1] at a wavelength of $\lambda_0 = 780\,\mathrm{nm}$ would result in a mode spacing of $\Delta\lambda \approx 0.05\,\mathrm{nm}$ which is drastically smaller compared to the typical width of tens of nano meters a quantum well laser is able to provide gain for[2]. Thus, for several longitudinal modes both threshold conditions may be fulfilled resulting in no stable longitudinal single mode operation at one wavelength or frequency. This can lead to multi mode emission and switching between modes, i.e. the occurrence of mode hops and may be triggered by spontaneous emission in the laser itself [Car+98] or due to the adaption of operating conditions as the maximum of the gain spectrum of the laser will be shifted when the temperature changes [Pip03] with a rate faster than the shift of the longitudinal modes due to temperature changes [HC93]. This includes increasing the injection current due to self-heating of the devices.

2.2 Externally stabilized and Distributed Bragg lasers

A straightforward way to make longitudinal single-mode operation possible is to use wavelength selective feedback. This can be realized with external feedback from a diffraction grating or a mirror in combination with another wavelength selective element [Mro08]. The idea is to make mirror losses α_m in Eq. (2.4) at all wavelengths different from that of the favored longitudinal mode sufficiently high such that only this mode

[1] e.g. compare experimental results in Ch. 5
[2] e.g. compare the spectrum in Fig. 6.11

reaches threshold. By extending the cavity, the photon lifetime in the cavity can be increased and the spectral linewidth decreased in comparison to bare FP diode lasers as well. However, by increasing the length of the external cavity L_{ext} which contains of material with the group index $n_{\mathrm{g,ext}}$ the mode spacing becomes even smaller. This becomes obvious from the generalized from of Eq. (2.6) [CCM12]

$$\Delta\lambda = \frac{\lambda_0^2}{2\left(n_{\mathrm{g}}L + n_{\mathrm{g,ext}}L_{\mathrm{ext}}\right)}. \tag{2.9}$$

I.e. the compound cavity supports an even higher number of longitudinal modes the wavelength selective filter has to suppress. In addition, the requirements on the opto-mechanics increases to guarantee stable operation. Though, it is possible to integrate the grating also monolithically to sections of the laser and form a wavelength selective mirror replacing and enhancing the function of one of the facets. The grating can be formed by a periodic corrugation of the refractive index near to the waveguide within the devices which are called distributed Bragg (DBR) lasers. The grating provides feedback with a maximum within a range around the wavelength λ_{Bragg} which met the Bragg condition [Car+98]

$$\lambda_{\mathrm{Bragg}} = \frac{2n_{\mathrm{eff}}\Lambda}{M} \tag{2.10}$$

where Λ is the grating period an M the order of the grating. The propagation constant at the Bragg wavelength according to Eq. (2.10) and Eq. (2.2), not considering gain or losses, is

$$\beta_{\mathrm{Bragg}} = \frac{\pi M}{\Lambda}. \tag{2.11}$$

A grating of length L_{grat}, a coupling coefficient κ, i.e. a measure proportional to the reflectivity of the grating per unit length, and that satisfies the Bragg condition provides a reflectivity of approximately [CCM12]

$$r = -\mathrm{i}\frac{\kappa\tanh\left(\sigma L_{\mathrm{grat}}\right)}{\sigma + \mathrm{i}\Delta\beta\tanh\left(\sigma L_{\mathrm{grat}}\right)} \tag{2.12}$$

when detuned from λ_{Bragg} which is accounted for by $\sigma^2 = \kappa^2 - \Delta\beta^2$ with the detuning parameter $\Delta\beta = \beta - \beta_{\mathrm{Bragg}}$. Unfortunately, in both classes of devices the tuning of the wavelength selective element and the gain spectrum of the laser diode are not generally synchronized when operation conditions are changed [Krü+19; Rad+11]. This leads to switching of the longitudinal modes. The mode-hop-free tuning range is in the order of the longitudinal mode spacing of the particular devices, however, only when carefully designed [Tro+18; Krü+19]. Although spectral tuning can be better controlled over a wide range by e.g. including an additional phase sections which has to be controlled appropriately [CC87] or synchronizing the wavelength tuning in the different sections of a DBR laser by a sophisticated mounting technology [YXI18] no inherently mode-hop-free tuning is possible for such device configurations.

2.3 Distributed feedback lasers

A solution to this problem is generally not to rely on a facet or single Bragg grating as mirror which provides necessary feedback but does not shift accordingly. Instead, it is possible to use only Bragg gratings to provide feedback. In the simplest case

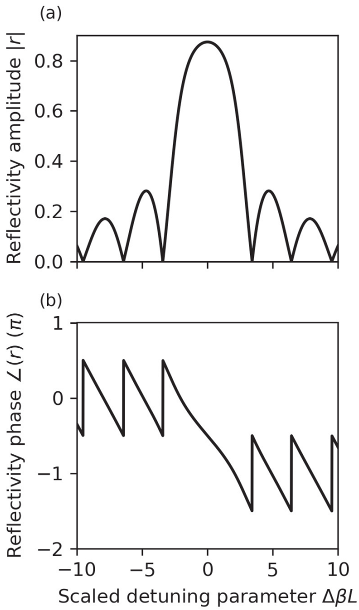

Figure 2.1: Panel (a) shows the reflectivity of a Bragg grating according to Eq. (2.12) with $\kappa = 4.5\,\mathrm{cm}^{-1}$ and a length of $L = 1500\,\mu\mathrm{m}$. The characteristics are plotted against the detuning parameter $\Delta\beta$ scaled by the grating length L. Panel (b) contains the corresponding phase of the reflectivity.

of a uniform grating that is integrated to a device which provides optical gain, two longitudinally counter propagating waves are coupled via the Bragg scattering of the grating. The Bragg grating provides feedback around the Bragg wavelength. Thus, there is no propagation at the Bragg wavelength and the scattered wave is just out of phase with the incoming wave as depicted in Fig. 2.2 (a). Another view to this problem and a possible way to identify solutions is to think of half of a period of the grating $\Lambda/2M = \lambda_{\mathrm{Bragg}}/4n_{\mathrm{eff}}$ being the smallest resonator in such a uniform structure if the Bragg condition is met. This resonator is surrounded by two Bragg mirrors. As the phase condition must be fulfilled by the DFB laser with uniform grating as well in analogy to the FP laser [CCM12; Car+98]

$$r^{\mathrm{front}}_{\mathrm{Bragg}} r^{\mathrm{rear}}_{\mathrm{Bragg}} \mathrm{e}^{-\mathrm{i}2\beta L} = 1 \tag{2.13}$$

must be satisfied with r^{front} and r^{rear} being the the reflection coefficients of the Bragg mirrors. Assuming the corrugation forming the Bragg gratings affect only the refractive index follows with Eq. (2.11) near to the Bragg condition $\beta \approx \beta_{\mathrm{Bragg}}$

$$r^{\mathrm{front}}_{\mathrm{Bragg}} r^{\mathrm{rear}}_{\mathrm{Bragg}} \mathrm{e}^{-\mathrm{i}\pi} = r^{\mathrm{front}}_{\mathrm{Bragg}} \mathrm{e}^{-\mathrm{i}\frac{\pi}{2}} r^{\mathrm{rear}}_{\mathrm{Bragg}} \mathrm{e}^{-\mathrm{i}\frac{\pi}{2}} = 1 \tag{2.14}$$

which must be satisfied. This is only possible, when r^{front} and r^{rear} are complex and provide an additional shift of $\exp\{\pm\mathrm{i}\pi\}$ in total or $\exp\{\pm\mathrm{i}\pi/2\}$ each. Comparing with the solution of Eq. (2.12) and Fig. 2.1 (b) there will be periodical solutions symmetrically placed around the Bragg wavelength which provide an appropriate phase shift. Suppressing any additional reflections from the facets by using AR coatings at least the two modes most near to the Bragg wavelength will reach threshold in such lasers. Thorough analysis using coupled mode theory [KS72] reveals that both modes will appear at $|\delta| \approx \kappa$. The approximation is used as the original publication was later extended to an effective index model which takes into account dispersion [Iga83]. The range in between is defined as stopband. I.e. such distributed feedback (DFB) lasers are in principle able to provide proper tuning but do not necessarily provide longitudinal single mode operation. However, several device configurations based on the general DFB laser design were investigated to overcome these shortcomings and guarantee single mode emission. A selection of approaches to solve the problem includes:

(i) Integration of a phase shift to the Bragg grating. For the obvious case of an additional phase shift $\Delta\phi_{\mathrm{ps}} = \pi$ Eq. (2.14) can be fulfilled at the Bragg wavelength. Such a phase shift equals just half of a period of the grating $\Lambda/2M = \lambda_{\mathrm{Bragg}}/4n_{\mathrm{eff}}$ and, thus, is called to be a quarter-wave phase shift (QWPS). It provides an additional path length of Λ/M. Phase shifts can be realized e.g. by directly writing

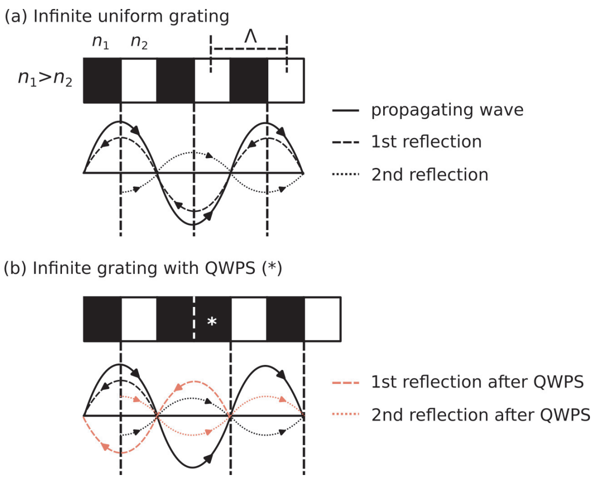

Figure 2.2: First and secondary reflections at a first order Bragg grating with grating period Λ and a refractive index modulation with sections of n_1 and n_2 which satisfy $n_1 > n_2$. The length of one section is $\Lambda/2 = \lambda_{\mathrm{Bragg}}/4n_{\mathrm{eff}}$. Reflections are shown for a uniform grating neglecting any effects from grating ends in panel (a) as well as for a corresponding grating with integrated quarter-wave phase shift (QWPS) in panel (b). Propagation at the Bragg wavelength is considered. For convenience a first order grating is shown. Panel (a) shows antiphase secondary reflections as expected from Eq. (2.14). The forward propagating wave is reflected. Its amplitude reduces during propagation. Panel (b) demonstrates in-phase secondary reflections after the QWPS making propagation of the wave possible around the phase shift.

them to the grating by adapting the corrugation pattern [Reg+24a], by modifying the wavequide and shifting the effective index locally [Sod+84; Abe+95] or by using locally chirped gratings to introduce distributed phase shifts [Hil+94a]. The additional phase shift does not necessarily be exactly $\Delta\phi_{\mathrm{ps}} = \pi/2$ to provide single mode operation since the symmetry in wavelength is abrogated as long as $\Delta\phi_{\mathrm{ps}} \neq 0$ and the mirror losses become sufficiently unequal for both modes most near to the stopband. However, this means other laser parameters as the wavelength of emission or the side mode suppression ratio (SMSR) become dependent on the actual phase shift as well. Fig. 2.2 presents first and secondary reflections for the cases of a uniform (a) and a first order Bragg grating around a QWPS (b) at the Bragg wavelength. The graphics demonstrate just anti- and in-phase secondary reflections which is in accordance with the lasing properties reviewed above.

(ii) Applying an AR coating to the front and a HR coating to the rear facet. This corresponds to introducing a phase shift at the HR coated rear facet for an otherwise uniform grating [SBS75; Hen85]. This design features a higher output power at the front facet in comparison to the rear facet. However, the cleaving position and thus the actual phase shift introduced cannot be controlled economically to a sufficient degree during processing. Similar to the considerations from (i) this will lead to varying laser parameters for otherwise similarly processed devices including the spectral behavior of the devices. A graphic representation of two prominent cases for mirror positions is given in Fig. 2.3. Panal (a) corresponds to a configuration in analogy to a DFB laser with a QWPS. Such a structure

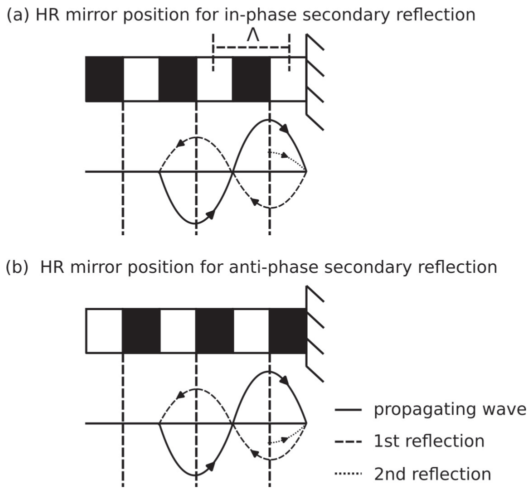

Figure 2.3: First and secondary reflections in a first order Bragg grating with a mirror at one end. In analogy to Fig. 2.2 first and secondary reflections are shown at the Bragg wavelength. (a) demonstrates a mirror position leading to in-phase secondary reflections and (b) a mirror position leading to anti-phase secondary reflections in analogy to a continued uniform grating.